Water–Air Interfaces

International Edition: DOI: 10.1002/anie.201411188
German Edition: DOI: 10.1002/ange.201411188

Molecular Structure and Dynamics of Water at the Water–Air Interface Studied with Surface-Specific Vibrational Spectroscopy

Mischa Bonn, Yuki Nagata, and Ellen H. G. Backus*

Keywords:
aqueous interface · molecular dynamics · time-resolved spectroscopy · sum-frequency spectroscopy · water–air interface

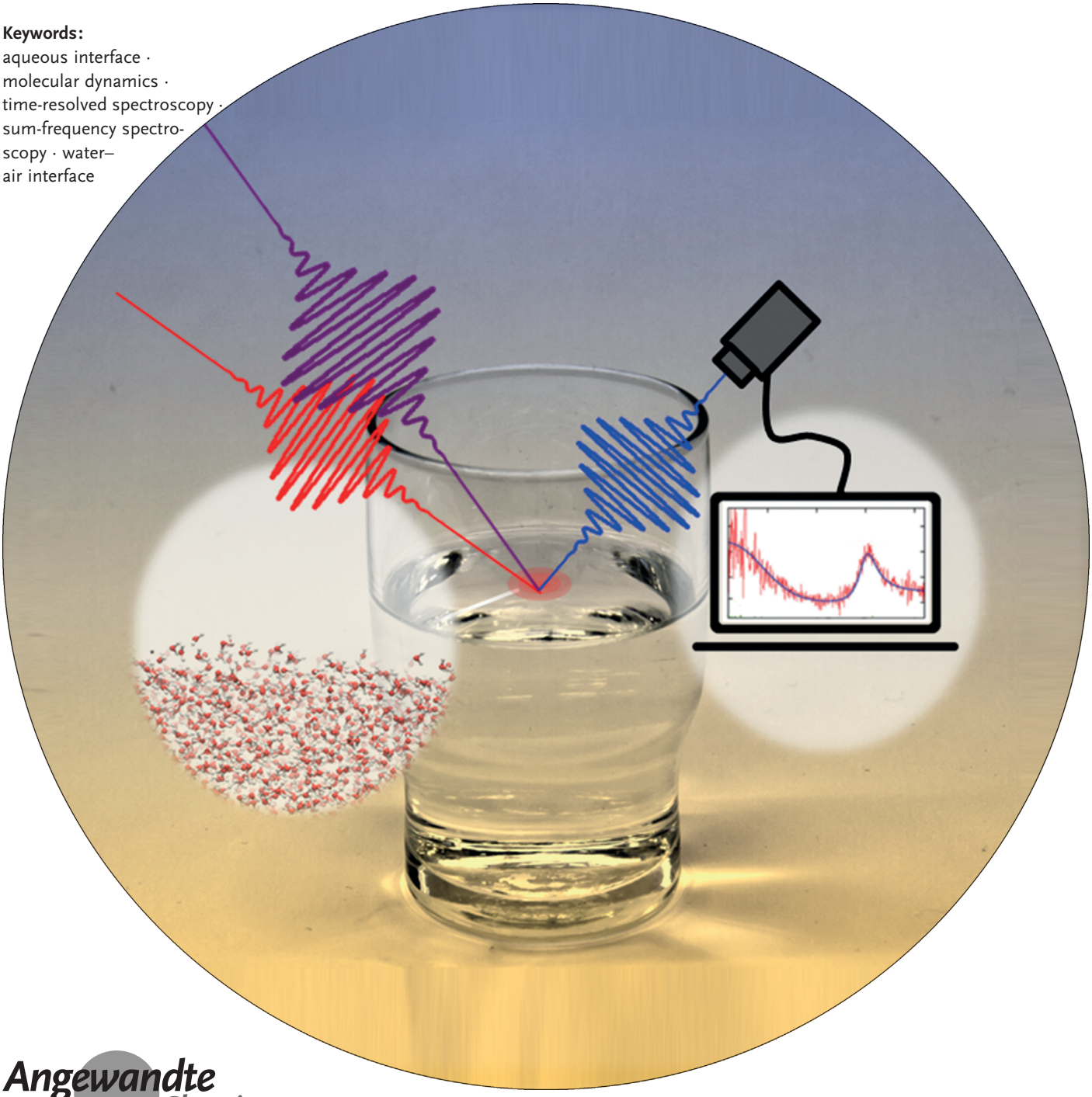

Water interfaces provide the platform for many important biological, chemical, and physical processes. The water–air interface is the most common and simple aqueous interface and serves as a model system for water at a hydrophobic surface. Unveiling the microscopic (< 1 nm) structure and dynamics of interfacial water at the water–vapor interface is essential for understanding the processes occurring on the water surface. At the water interface the network of very strong intermolecular interactions, hydrogen-bonds, is interrupted and the density of water is reduced. A central question regarding water at interfaces is the extent to which the structure and dynamics of water molecules are influenced by the interruption of the hydrogen-bonded network and thus differ from those of bulk water. Herein, we discuss recent advances in the study of interfacial water at the water–air interface using laser-based surface-specific vibrational spectroscopy.

From the Contents

1. Introduction

Water, H_2O, has a treacherously simple molecular structure. Yet an ensemble of water molecules has very unique properties that are difficult to predict from its molecular structure. The reason for this is that water is a highly collective liquid: very strong electrostatic intermolecular interactions occur between the partially positively charged hydrogen atoms on one water molecule with a partially negatively charged oxygen atom of another water molecule. These interactions are commonly denoted as hydrogen bonds. The collectivity originates from the fact that the presence of one hydrogen bond affects the structure and dynamics of water molecules beyond the two water molecules that are directly interacting. For instance, if a water molecule approaches a hydrogen-bonded water pair, the hydrogen-bond pair is exchanged through a transient conformation of a water "trimer", making one water molecule reorient.[1] Also, the hydrogen-bond strength between water molecules A and B affects the interaction energy between molecules B and C, that is, so-called many-body interaction effects are important in water.[2,3]

As a result of these strong intermolecular interactions and this collectivity, water differs markedly from liquids of similar molecular weight in properties, such as its high heat capacity, anomalous phase diagram, and the high dielectric constant of the bulk liquid. Moreover, the physical properties of interfacial water deviate in significant ways from bulk water.[163] For example, the dielectric constant of interfacial water is 10 times lower than the bulk, the surface tension of the water–air interface (relative to other liquids) is extremely high, and the phase diagram of interfacial water looks significantly different than that of the bulk water.[4,5] In addition to their fundamental interest, understanding these properties turns out to be critical in important topics, such as the discipline of electrochemistry, the surface chemistry of atmospheric aerosols, the chemistry of the mineral/water interface, and membrane biophysics, and small-scale phenomena, such as the movement of insects (i.e. water striders) over the water surface and the development of cracks in sidewalks on subfreezing days.[6–8]

Despite its importance, the understanding of interfacial water has lagged behind that of bulk water. In this Review we show in the first part how insights into the structure of interfacial water have been obtained by the surface-sensitive technique called sum frequency generation (SFG) spectroscopy. This Section is followed by time-resolved SFG experiments used to obtain information about the static structure but also about motion and structural dynamics of the molecules in real time. Subsequently, it is illustrated how the time-resolved experiments provide details about the energy flow in the system. We conclude with an outlook. As interfacial water is a very broad topic, this Review cannot cover the whole field. We therefore limit ourselves to the planar water–air interface, as a special case of water at hydrophobic interfaces, although lately much interesting work has been done on water at hydrophobic interfaces in general. The interested reader is referred to the corresponding literature.[9–17] In the outlook we briefly discuss water at other interfaces.

2. Method: Interface-Specific SFG Spectroscopy

It is highly challenging to characterize the outermost monolayer of water at an interface. Even for very thin

[*] M. Bonn, Y. Nagata, E. H. G. Backus
Max-Planck-Institut für Polymerforschung
Abteilung für Molekulare Spektroskopie
Ackermannweg 10, 55128 Mainz (Germany)
E-mail: bonn@mpip-mainz.mpg.de

samples—say 1 μm thin—the number of water molecules in the few Å thin interfacial region is many orders of magnitude smaller than that in the 1 μm "bulk" below the surface. Conventional techniques that provide direct information on structure, such as X-ray and neutron scattering and absorption, are useful for probing the structure of bulk liquid water,[18,19] but require special experimental geometries to extract information about the interface.[20–22] In the majority of geometries the signal from the, relatively small, number of water molecules at the interface is dwarfed by that from the much larger number of molecules in bulk.

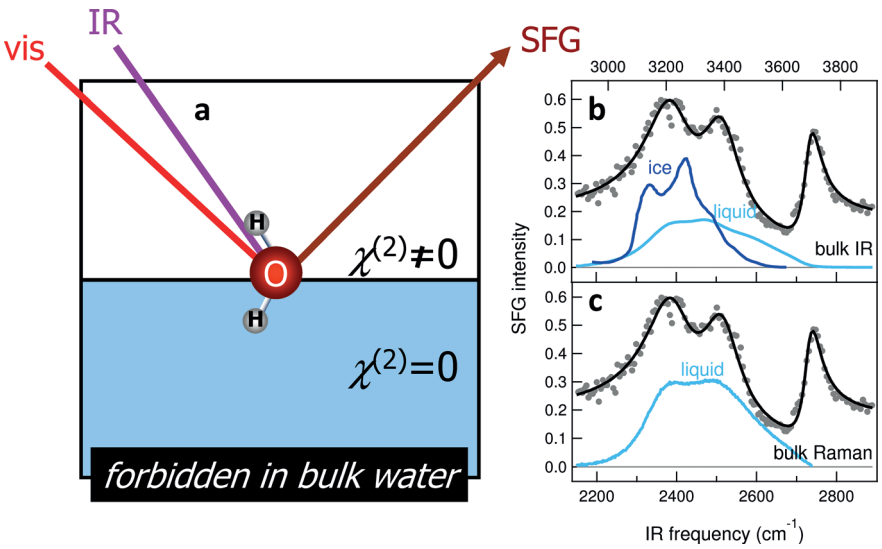

Figure 1. a) Principle of an SFG experiment b) SFG spectrum of the D_2O–air interface (gray circles, black line to guide the eye) together with a bulk IR spectrum of D_2O ice (dark blue) at −173 °C[47] and an attenuated total reflection IR spectrum of D_2O liquid (light blue). c) Depolarized Raman spectrum of liquid D_2O. The SFG spectrum from panel (b) is replotted. The top axis uses the frequency of the bottom axis multiplied by 1.37 times, which corresponds to the O-H stretch frequency.

While direct elucidation of interfacial water organization is thus difficult, there is an alternative approach. The structure of bulk liquid water strongly depends on its hydrogen-bonded network. Therefore, we might expect to learn about the interfacial water structure if we examine the strength and manner of water's hydrogen-bond interactions. This is an alternative approach to directly probe the relative position of water molecules. The central frequency and lineshape of the O–H stretch vibration (in H_2O) is sensitive to the hydrogen-bond strength and topology.[23] Specifically, an O–H···O hydrogen bond strength governed by the intermolecular H···O distance and angles of the acceptor orientation[24] weakens the covalent O–H bond of the hydrogen-bond donor, lowering the O–H stretch vibrational frequency. Therefore, the hydrogen-bond-induced shift in the O–H stretch frequency can be directly correlated to the hydrogen bond energy. Conventional one-dimensional (1D) infrared (IR) absorbance and Raman scattering spectroscopies have provided a variety of insights into the local hydrogen-bonding properties of bulk liquid water under various conditions[25–27]—but these techniques are not surface specific. To obtain the information on the structure and hydrogen-bond network of the interfacial water molecules, the vibrational frequency of the water molecules specifically at the interface has to be measured.

The Shen group, and since then a variety of others, recognized that this could be done by using vibrational sum frequency generation (SFG) spectroscopy: an experimental scheme in which a pulsed IR and pulsed visible beam are overlapped in space and time at an interface and the resulting emission of photons at the sum of the two frequencies is measured (see Figure 1 (a)).[28–46]

Symmetry selection rules for the sum frequency process dictate that there are no sum frequency photons emitted from bulk water where the net orientation of water molecules along the surface normal is zero, while the sum frequency emission strongly increases as the IR frequency is scanned over a vibrational resonance of interfacial water molecules, for which the symmetry is broken.[164] Hence, SFG can be an interface-specific vibrational spectroscopy in which the vibrations of water are used as reporters on its local structure. The

Yuki Nagata is a group leader at Max-Planck Institute for Polymer Research (MPIP), Mainz, Germany, and works on the molecular dynamics simulation of surface-specific vibrational spectroscopy at the aqueous interfaces with. He received his Ph.D. from Kyoto University, Japan, on simulation of two-dimensional vibrational spectra for the liquid/solid/surface systems. After a research position at BASF Ludwigshafen, Germany, and a postdoctoral stay with Prof. Shaul Mukamel, University of California, Irvine, USA, he joined the MPIP. His main research interests are the interfacial water and theory of the vibrational surface spectroscopy.

Mischa Bonn is a director at the Max-Planck Institute for Polymer Research (MPIP), Mainz, Germany. He works on label-free (ultrafast) vibrational spectroscopy and microscopy of biomolecular systems and water in such systems. He received his PhD in 1996 from the University of Eindhoven for research performed at the AMOLF in Amsterdam. After postdoctoral research at the Fritz Haber Institute in Berlin and Columbia University in New York, he worked at Leiden University from 1999 as an assistant then associate professor. In 2004 he became a group leader at the AMOLF. In 2011 he joined the MPIP. His research interests are the structure and dynamics of molecules at interfaces, and electron transfer across interfaces.

exact probing depth of SFG depends on the characteristics of the interface. Of course, if the surface is charged, for example, SiO_2 in contact with water at neutral pH, the symmetry will be broken over a larger depth into the water compared to a neutral interface. For the water–air interface, the focus of this Review, the probing depth is 5 Å at most, corresponding to 1–2 monolayers of water. This value is obtained from molecular dynamics (MD) simulations showing that there is no preferential water orientation deeper than 5 Å and that the calculated SFG spectrum does not change anymore by including water below 5 Å from the air–water interface.[48,49]

With conventional IR spectroscopy it has been observed that upon changing from the gas to condensed phases, the symmetric and antisymmetric modes at 3657 (2672) and 3756 (2788) cm^{-1}, respectively, generated by the two O–H (O–D) groups in a single water molecule collapsed to the broad band centered at approximately 3350 (2450) cm^{-1} in liquid water and approximately 3200 (2350) cm^{-1} in ice (see Figure 1b). Intriguingly, an SFG vibrational spectrum of the water–air interface, first reported by Shen and co-workers[29] and subsequently by many others showing a very similar spectrum,[50] appears to have all three of these modes: the peak at approximately 3700 (2750) cm^{-1} is generally assigned to water molecules with one O–H group pointing into the gas phase and termed the "free O–H" group, while the peaks at approximately 3200 (2350) and approximately 3400 (2500) cm^{-1} appear in the frequency region for hydrogen-bonded O–H groups. These latter two peaks originate from the majority of water molecules at the interface, which donate two hydrogen bonds. In analogy to the IR absorption spectrum of ice and liquid water, these two peaks in the SFG spectrum have, over the last fifteen years, been taken to be the result of "ice-like" and "liquid-like" interfacial water.[29,30,33–35,51–53] As will be shown below, recent work has demonstrated that there is no evidence for "ice-like" and "liquid-like" interfacial water species at the water–air interface. The water interface is indeed more heterogeneous than bulk water, but not because of the presence of more strongly coordinated, "ice-like", O-H groups at the interface. Rather, some of the interfacial water molecules are in fact undercoordinated, giving rise to relatively weak hydrogen bonds at the interface. Below, we provide experimental evidence for a sub-ensemble of relatively weakly hydrogen-bonded O-H groups that is largely decoupled from other O-H groups, and that is specific to the interface.

Ellen Backus is a group leader of the "Water at Interfaces" group in the Molecular Spectroscopy department at the Max Planck Institute for Polymer Research (MPIP), Mainz, supported by a Minerva Grant from the Max Planck Society, and an ERC Starting Grant. She obtained her PhD in 2005 at Leiden University in the group of Mischa Bonn and Aart Kleyn. After a PostDoc at the University of Zurich with Peter Hamm, she moved back to the Netherlands for an independent PostDoc position in the group of Huib Bakker at the AMOLF in Amsterdam. In 2012, she joined the MPIP. Her research is in the structure and dynamics of water at various interfaces.

3. The Structure of Interfacial Water

While it is tempting to assign the peaks emerging in the SFG spectrum at the water–air interface to specific types of water molecules present at the interface, it is not evident that this can be done simply. More specifically, the presence of "ice-like" water at the water–air interface at room temperature seems to contradict what we know from the thermodynamics of water. Since the first discovery by Faraday, it has been established that below the bulk freezing point of water, a thin layer of liquid water coats the ice surface.[54] This would make an "ice-like" structure of liquid water above the bulk freezing point thermodynamically not viable. On the other hand, the similarity of the SFG signal to the combined IR responses of bulk ice and liquid water seems to make a strong case for ice-like and liquid-like structures at the water–air interface. How can this apparent contradiction be lifted? It is important to realize that the SFG signal cannot be compared directly to the IR response. It is the second-order nonlinear susceptibility $\chi^{(2)}_{abc}$ at the *abc* polarization direction (*a*: SFG signal polarization direction, *b*: visible-light (Vis) polarization direction, *c*: IR polarization direction) that determines the SFG intensity spectrum, through [Eq. (1)].

$$I(\omega_{SFG}) \approx \left|\chi^{(2)}_{abc}\right|^2 I_{IR}(\omega_{IR}) I_{VIS}(\omega_{VIS}) \quad (1)$$

That is, the SFG intensity is proportional to the intensity of the incident IR and visible beams, and to the square of the second-order susceptibility $\chi^{(2)}_{abc}$. The complex quantity $\chi^{(2)}_{abc}$ contains the information about the vibrational response of the interfacial water molecules, since it is proportional to the product of their transition dipole moment and polarizability [Eq. (2)]

$$\chi^{(2)}_{abc} \approx \sum_i \frac{\partial \mu_c}{\partial Q_i} \cdot \frac{\partial \alpha_{ab}}{\partial Q_i} \quad (2)$$

where μ is the dipole moment, α the polarizability, and Q_i the *i*th normal mode of the molecules.[55] $\partial\mu/\partial Q$ and $\partial\alpha/\partial Q$ are the IR transition dipole moment and the Raman transition polarizability tensor, respectively. It is therefore clearly justified to compare the SFG response of interfacial water to the IR response of bulk water (through the term $\partial\mu_c/\partial Q$), yet the Raman response ($\partial\alpha_{ab}/\partial Q$) is equally important in determining $\chi^{(2)}_{abc}$. Remarkably, the Raman response of bulk water (Figure 1c) shows the same double-peaked feature as observed in the SFG spectrum in the hydrogen bonded region (for H_2O 3100–3500 cm^{-1}, for D_2O 2300–2600 cm^{-1}). The double-peaked Raman feature has been ascribed to both intramolecular[56–58] and intermolecular coupling of the O–H stretching modes.[25,51,52] Intramolecular coupling originates from splitting of the degenerate vibrational energy levels of the O–H stretch mode and the overtone of the water bending mode (Fermi resonance). Since these two modes have similar

vibrational energy levels, their anharmonic interaction splits these energy levels into a low- and a high-frequency band, providing an explanation for the double-peaked feature in the SFG spectrum (see Figure 2b). Intermolecular coupling, in contrast, results in the transfer of vibrational energy between

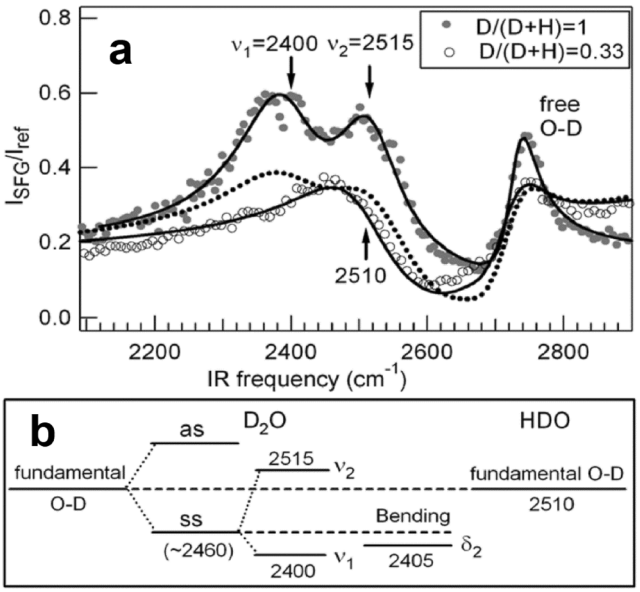

Figure 2. a) SFG spectra (SSP polarization) of the water–air interface for both pure (closed symbols) and isotopic diluted (open symbols) D_2O. The solid black lines are fits to the data and a simulated spectrum for the "ice- and liquid like" hypothesis is shown by the black dotted line. b) Energy levels for D_2O and HDO water molecules illustrating the effect of coupling. Owing to intramolecular coupling the fundamental O–D stretch vibration is split into a symmetric (ss) and asymmetric (as) mode. The ss mode is further split into ν_1 and ν_2 through coupling with the overtone of the bending mode (δ_2) and/or intermolecular coupling effects. In an HDO molecule these intramolecular coupling effects are switched off. The intermolecular coupling is also reduced. Therefore the fundamental O–D stretch vibration can be determined. The mode frequencies are given in cm^{-1}. Reprinted with permission from Ref. [60]. Copyright 2008 by the American Physical Society.

different water molecules and, as such, can affect vibrational lineshapes by creating additional intensity at the low-frequency side of the spectrum. Based strictly on the analogy to the bulk Raman spectrum, it might be argued that there is no such thing as separate "ice-like" and "liquid-like" types of interfacial water and that, in general, the hydrogen-bonding environment at the interface is similar to that in the bulk.

The presence—or absence—of "ice-like" and "liquid-like" interfacial substructures can be explored experimentally. If distinct substructures were present at the interface, this implies the presence of weak "liquid-like" and strong "ice-like" hydrogen bonds. This variation in hydrogen-bond strengths should be independent of the hydrogen/deuterium (H/D) isotopic composition of the water investigated in the experiment. Such isotopic dilution experiments were first performed by the Richmond group.[35,59] The rationale was, that for all H_2O, HDO, and D_2O the two peaks should be present. If, in contrast, the presence of the two peaks is due to coupling, be it between stretching and bending modes (intramolecular coupling) or between different water molecules (intermolecular coupling), the two-peak response should vanish when going from H_2O, or D_2O to HDO: in HDO, the effect of intramolecular coupling is "switched off" since the overtone of the bending mode is no longer degenerate with either the O–H or the O–D stretch mode within the HDO molecule. Isotopic dilution also reduces the effect of intermolecular coupling, as it reduces the effective density of, respectively, O–H and O–D groups.

Indeed, it could be demonstrated that the double-peaked SFG feature disappears when water is isotopically diluted (Figure 2).[60] This observation is inconsistent with "ice-like" and "liquid-like" interfacial substructures, which should persist upon isotopic dilution from H_2O to HDO. Hence, it is evident that no "ice-like" structures are present at the water–air interface. This conclusion was later confirmed for other types of aqueous interfaces as well.[61–63] Finally, we note that simulations combined with calculations of the surface spectroscopy, have indicated that it is the intermolecular, rather than the intramolecular coupling that is primarily responsible for the observed spectral changes upon isotopic dilution.[2,25,64–66]

In the SFG experiments described above, the SFG intensity, $|\chi^{(2)}|^2$, was reported. However, $\chi^{(2)}$ is a complex parameter, and it is the imaginary part of $\chi^{(2)}$, $\mathrm{Im}[\chi^{(2)}]$, which can be directly compared with, for example, the linear IR and Raman spectra of water. Moreover, the $\mathrm{Im}[\chi^{(2)}]$ signal can be positive or negative, which provides information on the absolute (up or down) orientation of the interfacial water molecules along the surface normal. This information is missing in the $|\chi^{(2)}|^2$ intensity spectrum. Figure 3 displays the

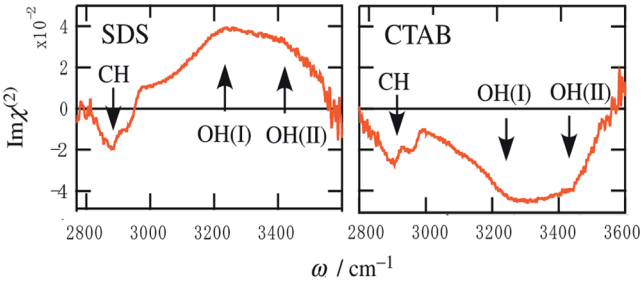

Figure 3. $\mathrm{Im}[\chi^{(2)}]$ spectra of the water–air interface underneath a monolayer of the negatively charged surfactant (SDS) and the positively charged surfactant (CTAB). CH denotes the CH_3 stretching bands of the surfactants, while OH(I) and OH(II) mark the different water O–H stretch vibrational bands. Reprinted with permission from Ref. [67]. Copyright 2009, AIP Publishing LLC.

$\mathrm{Im}[\chi^{(2)}]$ signals of the O–H stretch modes near a negatively charged (sodium dodecyl sulfate, SDS) and positively charged (cetyltrimethylammonium bromide, CTAB) surfactant monolayer. These spectra show the opposite signs for the O–H stretch bands, clearly demonstrating that the water orientation is opposite for a positive and a negative charged surfactant.[67]

To obtain the complex $\chi^{(2)}$ signals, a phase-sensitive SFG experiment has to be performed. In this technique, the SFG signal is mixed with a signal of known, constant phase, allowing the determination of the frequency dependent phase of the SFG signal through the interference of the two signals. Phase-sensitive detection of SFG signals was first reported by

Shen and co-workers,[38,68] while a method using broad-bandwidth laser pulses was first developed by Tahara and co-workers, which was termed heterodyne-detected (HD-) SFG.[67] Figure 4 displays the Im[$\chi^{(2)}$] signals at the water–air interface.[62,69] The spectrum of neat H_2O/air interface (blue line in the top panel of Figure 4) shows the same three

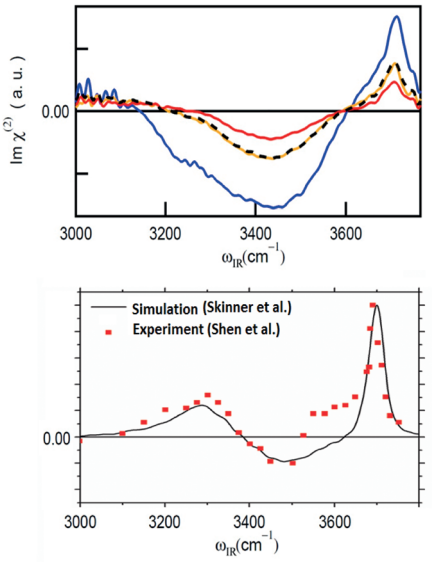

Figure 4. Top: Im[$\chi^{(2)}$] signal for the water–air interface with various isotope dilutions: pure H_2O (blue), H_2O:HOD:D_2O = 2:5:3 (yellow) and 1:6:9 (red). The black dotted line is the yellow spectrum calculated from a linear combination of the blue and red curves. Reprinted with permission from Ref. [62]. Copyright 2011 American Chemical Society. Bottom: The simulated Im[$\chi^{(2)}$] with the three-body potential model and experimentally measured Im[$\chi^{(2)}$] for the HOD–air interface.[69] Reprinted with permission from Ref. [2]. Copyright 2011 American Chemical Society.

features apparent in the intensity spectrum: a sharp 3700 cm^{-1} positive peak corresponding to the free O–H group pointing up into the air, and broad negative peaks at 3400 cm^{-1} and 3200 cm^{-1} assigned to the hydrogen-bonded O–H group pointing down to the bulk. A fourth, relatively weak, positive band is observed at 3100 cm^{-1}, which is not directly apparent from the intensity spectrum and the origin of which has been debated. Upon isotopic dilution, the peak at 3200 cm^{-1} disappears and the hydrogen-bonded signals merge into one peak, with a frequency in between the 3200 and 3400 cm^{-1} signals, closer to 3400 cm^{-1}, in good agreement with the SFG intensity spectra discussed above: The intra- and intermolecular coupling decreases upon isotopic dilution resulting in a simpler spectrum. Thus, the phase-resolved measurements confirmed the absence of "ice-like" structures at the interface of water.

To explore the molecular origin of the 3100 cm^{-1} peak, which is not so apparent in the intensity spectrum but clearly in the Im[$\chi^{(2)}$] spectrum, molecular dynamics (MD) simulations have been employed. By modifying the electrostatic interaction for calculating the optical response, Ishiyama and Morita showed that this 3100 cm^{-1} feature arises from the induced dipole moment through the anisotropic component of the polarizability of the interfacial water molecule.[70,71] In this approach, the induced dipole moment and polarizability can be calculated directly from the local structure, while three-body interactions are missing. Skinner and co-workers performed an MD simulation with their force-field model including the three-body interactions and attributed the positive feature mainly to water molecules forming four hydrogen bonds.[2,69,72] In this case, however, with their mapping methodology, the orientations of the transition dipole moment and polarizability are rather arbitrary. Irrespective of the detailed explanation, neither of the simulations provides any evidence for an ordered ice-like structure present at the liquid-water–air interface. Although heterodyne, phase-resolved methods unequivocally provide a more definitive way of determining the surface vibrational response of water, the corresponding Im[$\chi^{(2)}$] spectra still leave room for interpretation of the details of the interfacial water structure.

An very elegant test for hydrogen-bond strength at the water–air interface has been performed by Benderskii, Skinner, and co-workers.[73] Their isotopic dilution spectroscopy shows that the free O–D group at the water–air interface is coupled to the other hydrogen-bonded O–D group of the same water molecule. This is clear from the frequency shift observed for varying H/D concentrations (see Figure 5). From the coupling strength of 17 cm^{-1}, they estimated a hydrogen-bonded O–D frequency of 2580 cm^{-1}, which is close to the bulk IR peak frequency of 2480 cm^{-1}. This result demonstrates that the hydrogen-bond strength of interfacial water is similar to that of bulk water.

In summary, these isotopic dilution experiments seem to indicate that the averaged hydrogen-bond strength at the water interface closely resembles that of the bulk liquid water. The question that thus remained, was: Is the structure of interfacial, hydrogen-bonded water completely bulk-like? If this is true for the average response of interfacial water, then to what extent is the fluctuation of the interfacial hydrogen-bonding structure different from that of bulk water? How heterogeneous are water molecules at the interface?

Very similar questions about the hydrogen-bond structure of water have been raised previously for bulk water, where, similarly, static vibrational spectroscopy does not provide direct, unambiguous information about the water structure. For bulk water, these questions have been successfully addressed using pulsed, intense mid-IR lasers, allowing for mid-IR pump/probe and multidimensional IR spectroscopy.[74–81] In these experiments, the vibrational ground state is depleted by an initial pulse of intense IR radiation and the rate of repopulation on this ground state is probed by a temporally delayed IR pulse. These techniques have allowed detailed insights into the structure and structural dynamics of liquid water and aqueous solutions (see for example, Refs. [82–84] for details). Recently, these techniques have also been implemented for interfacial water. By monitoring the O–H stretch vibration of water, and making use of the correlation between its vibrational frequency and the hydrogen-bonding strength,[23] the temporal evolution of O–H stretch vibrational dynamics has yielded valuable insight into (sub-)picosecond water structural dynamics as

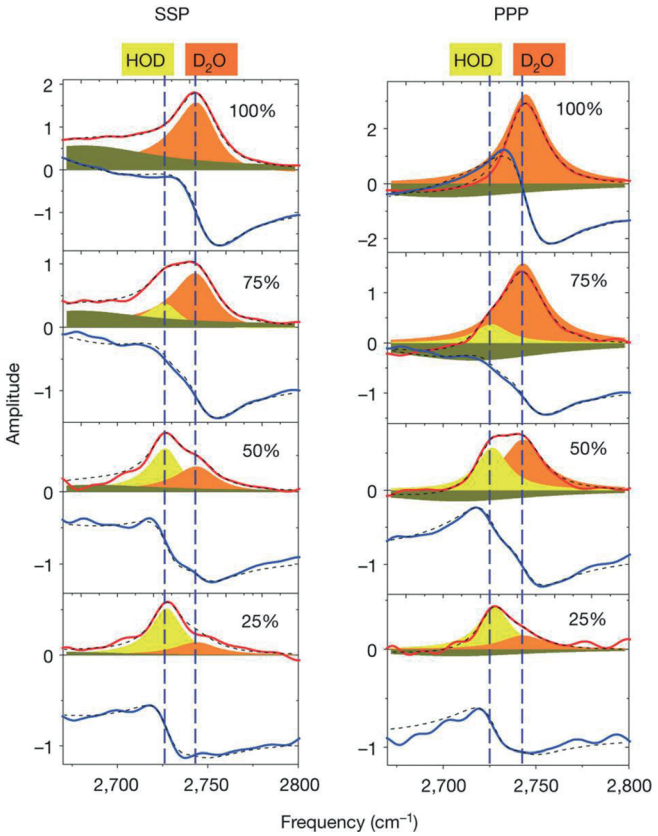

Figure 5. HD-Im[$\chi^{(2)}$] of the free OD stretch vibration for different isotopic mixtures H_2O:HOD:D_2O at the SSP (left) and PPP (right) polarizations. The D/H mole fraction is indicated. Blue and red lines are the experimentally measured real and imaginary parts of the SFG signal. Dashed lines are fits to a sum of Lorentzian terms and a non-resonant background. Shaded orange and yellow peaks indicate the free OD stretch mode of, respectively, D_2O and HOD molecules. Reprinted by permission from Macmillan Publishers Ltd: Ref. [73] copyright 2011.

well as into the structure of interfacial water, which will be detailed below.

4. Insights into the Structure of Interfacial Water from Time-Resolved Measurements

To elucidate the structure of interfacial water in more detail, surface-specific versions of mid-IR pump/probe and multidimensional IR spectroscopies have been developed.[11,85–95] In these experiments, a specific sub-set of water molecules is vibrationally excited, that is, "tagged", with an intense, femtosecond IR pulse (Figure 6a).

The excitation leads to a transient decrease in the SFG signal (Figure 6b), as excited interfacial O–H groups cannot generate SFG intensity at the fundamental frequency. Specific subsets of weakly (strongly) hydrogen bonded water molecules can be excited, by exciting the red (blue) sides of the IR response of the interfacial water molecules. The response of the water molecules is probed across a very wide frequency range (Figure 6c), and can be recorded as a function of time τ after excitation. From the probe spectra taken with different excitation frequency, 2D spectra can be constructed. The intensity of the signal change as a function of excitation and detection wavelength is depicted in such plots, in analogy to 2D-IR[78,96] or 2D-NMR.[97] See Ref. [98,99] for a detailed comparison.

Two limiting cases that can occur in 2D-SFG spectroscopy are shown in Figure 7a,b. For the limit that all O–H stretch chromophores are indistinguishable (i.e. the hydrogen bonds of the interfacial water are completely homogeneous) the response of the interfacial water molecules is independent of the precise excitation wavelength. As a result, the transient spectrum appears similar for all excitation frequencies and is elongated along the excitation frequency axis (Figure 7a). If, in contrast, distinct sub-ensembles of water (e.g. "liquid-like" and "ice-like" interfacial water) exist, the vibrational responses are governed by inhomogeneous broadening, and the vibrational response would primarily occur at the excitation frequency, so that the 2D-SFG spectrum will be elongated along the diagonal (Figure 7b). Furthermore, distinct sub-ensembles could result in two peaks at distinct frequencies along the diagonal line as well as (off-diagonal) cross peaks for these frequencies (Figure 7c). The presence of the cross peaks indicates that these vibrational modes are coupled. Such coupling can be associated with, for example, energy transfer or structural fluctuations.

Figure 7d shows the 2D-SFG spectrum recorded at the D_2O–air interface. The spectrum consists of a broad feature along the diagonal in the hydrogen-bonded O–D stretch region (between 2250 and 2650 cm^{-1}) and a narrow feature at 2750 cm^{-1} originating from the free O–D group. Moreover, cross peaks are visible between the free O–D peak and the high frequency side of the hydrogen bonded peak, as indicated by circles in the 2D spectrum. The diagonal peak in the hydrogen-bonded O–D stretch frequency looks very similar to the schematic for the homogeneous limit (Fig-

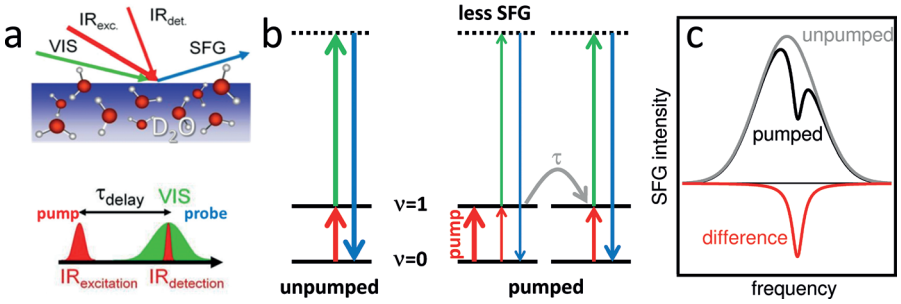

Figure 6. Geometry (a), energy-level diagram (b), and schematic of a spectrum (c) for an IR-pump SFG-probe experiment. The ground-state population is decreased by pumping part of the population to the excited state (b), giving rise to the reduction of the signal at the pump frequency. Relaxation processes can be probed by varying the waiting time τ between pumping and probing. The differential spectrum (red line in (c)) directly reflects the degree of heterogeneity of the water surface.

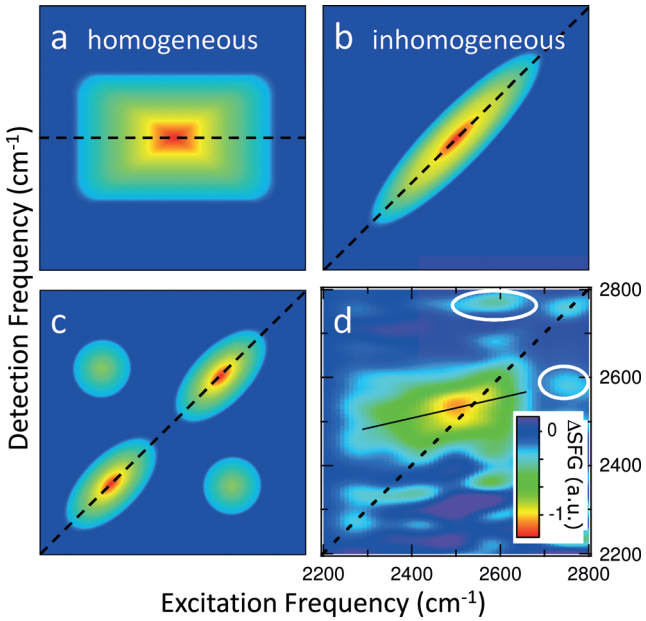

Figure 7. Schematic representation of a 2D spectrum in a) the fully homogeneous and b) inhomogeneous limit. c) A schematic representation of the 2D spectrum of an ensemble of two species with coupling between them. The coupling gives rise to the observed off-diagonal intensity. d) 2D-SFG spectrum of the water–air interface at zero time between pump and probe pulses.[100] Circles indicate (reproducible) off-diagonal intensity in the spectrum, which testifies to coupling between the free OH groups and weakly hydrogen-bonded O–H groups.[72]

ure 7a), confirming the earlier conclusion that no "ice-like" and "liquid-like" structures of water exist at the water–air interface.[60] The observed elongation along the excitation frequency axis can be understood from the different selection rules along the detection (IR and Raman activity required) and excitation (only IR activity required) axes.

Moreover, the 2D-SFG spectrum for hydrogen-bonded O–D vibrations shows a very similar response to that observed in 2D-IR experiments performed on bulk liquid water,[101,102] indicating that hydrogen-bonded interfacial water is fairly similar to bulk liquid water. This picture was refined in a later set of more advanced SFG experiments, HD-2D-SFG experiments on H_2O.[92,94] These 2D-SFG experiments confirmed that the frequency diffusion for most of the O–H stretch chromophores of the hydrogen-bonded interfacial water is slightly slower (240 fs)[94] than the bulk water (180 fs).[102] This slow-down was attributed to a reduction in the near-resonant vibrational energy transfer between different O–H groups, as a result of the effectively reduced density at the water–air interface owing to the truncation of the hydrogen-bond network. In addition to these "bulk-like" O–H groups, a distinct sub-ensemble of weakly hydrogen bonded O–H groups was identified at the water–air interface. Remarkably enough, despite being undercoordinated compared to the more strongly hydrogen-bonded water, and therefore structurally less confined, the structural dynamics of these weakly hydrogen-bonded O–H groups was found to be rather slow.

In summary, our understanding of the structure of interfacial water at the water–air interface has evolved considerably over the past few years: initial SFG experiments clearly showed the presence of the free O–H, sticking out into the gas-phase. This conclusion has been firmly reestablished by subsequent experiments. However, the initial proposition that, in addition to "liquid-like" water, also "ice-like" water exists at the water–air interface, was not apparent from later data. Rather, the most recent experiments have shown that in addition to "liquid-like" interfacial water, less-strongly hydrogen-bonded water molecules exist at the interface. Given the interruption of the hydrogen-bonded network at the water–air interface, the presence of more-weakly (rather than more-strongly "ice-like") hydrogen-bonded water at the interface seems intuitive.

While for the water–air interface there thus seems to be little indication for enhanced hydrogen bonding at the interface, we note that for water in contact with hydrophilic solid interfaces that can accept and/or donate hydrogen bonds, the presence of water that is hydrogen-bonded more strongly than in bulk, can certainly not be excluded.

5. The Dynamics of Interfacial Water

In addition to the structural parameters, information on the water dynamics is essential for understanding the processes of hydrogen-bond formation and breaking, specifically at the interface. This information can be obtained from time-resolved SFG experiments. Following the excitation ("tagging") of specific O–H groups at the water interface as described in the previous Sections, the subsequent structural changes in the water interfacial hydrogen-bonded network can be monitored in real-time by measuring SFG spectra at (sub)picosecond time delays.

The timescale on which the O–H stretch chromophores change their frequency and their orientation provides rather direct information on the hydrogen-bond dynamics. In this Section we discuss the structural and vibrational dynamics of both the free O–H and the hydrogen-bonded water. Finally, we show how the ultrafast dynamics of interfacial water can be used to obtain new information on the interfacial structure of aqueous salt solutions. In particular, we show how the slowdown of energy transfer at the interface of ionic solutions can be directly related to an excess of anions at the water interface.

5.1. The Dynamics of Free O–H Groups at the Water–Air Interface

The presence of the vibrational SFG signature of free O–H groups is characteristic of hydrophobic interfaces, such as the water–air interface, although free O–H groups do not appear for all hydrophobic interfaces.[14,103] The free O–H groups at the water interface play an important role in hydrophobic hydration assembly[104–106] and on-water catalysis.[107] For these catalytic and hydration processes involving the free O–H groups, the dynamics of the free O–H groups is

a key factor. Specifically, the rate at which excess energy is dissipated from the surface into the bulk is relevant for chemistry occurring at the surface. Moreover, the reorientational dynamics of the free O–H groups is important in understanding hydrophobic hydration at aqueous interfaces. Femtosecond time-resolved SFG spectroscopy allows the dissipation of the excess vibrational energy to be followed, as well as the structural dynamics of interfacial water, in real time. As the free O–H stretch mode at 3700 cm^{-1} is spectrally well separated from the hydrogen-bonded O–H stretch modes as we have seen above, it can be vibrationally excited—and probed—separately from its hydrogen-bonded counterparts.

The first question concerning structural dynamics of the free O–H groups is the timescale and mechanism of their reorientation. As opposed to molecular reorientation in most liquids, water reorientation in the bulk liquid is a highly non-diffusive process owing to the hydrogen-bonded network.[1] For a water molecule to reorient, at least one hydrogen-bond has to be broken with a hydrogen-bonding partner, and another hydrogen bond with a new partner formed. The substantial energetic cost of breaking a hydrogen bond prohibits this reorientation from occurring as a sequential process. Rather, the new hydrogen-bonding partner has to approach the water molecule that is about to reorient, and the transition state for the reorientational motion is a bifurcated hydrogen bond: for a short period of time (approximately 100 fs) the water molecule that reorients, is over-coordinated with one of its O–H groups transiently donating two hydrogen bonds. The "old" hydrogen bond can then be broken, and the "new" one can be firmly established. The net result is a reorientation of the water molecule, which occurs with a time constant of approximately 2.5 ps.[108] As a result, the rotational motion of water molecules in bulk is non-diffusive and occurs through a jump-like reorientation mechanism.

It is interesting to compare the reorientation of water molecules in bulk with those at the interface. Specifically, the free O–H group at the water interface is not hydrogen bonded, and therefore it may be expected to undergo both faster reorientation, as well as more diffusive-type behavior. Moreover, at the interface the symmetry is broken, and in-plane and out-of-plane motion could be expected to be quite different.

The reorientation of free O–H groups at the water–air interface was measured using time-and polarization-resolved sum frequency generation spectroscopy.[90] The basic idea behind these experiments is that, for a given (S or P) polarization of the excitation pulse, preferentially those O–H groups that are aligned along the polarization axis will be excited. This will give rise to an anisotropic distribution of excited ("tagged") and unexcited O–H groups. The SFG signal for P excitation and P probing is thus larger than for S excitation and P probing, as can be seen in Figure 8a. The "tagged" O–H groups will subsequently reorient, causing the memory-loss of the orientations of the O–H groups in time. Using an appropriate model, the different signal decays under the S- and P-pump polarization direction can be related to the reorientational motion of the O–H groups.

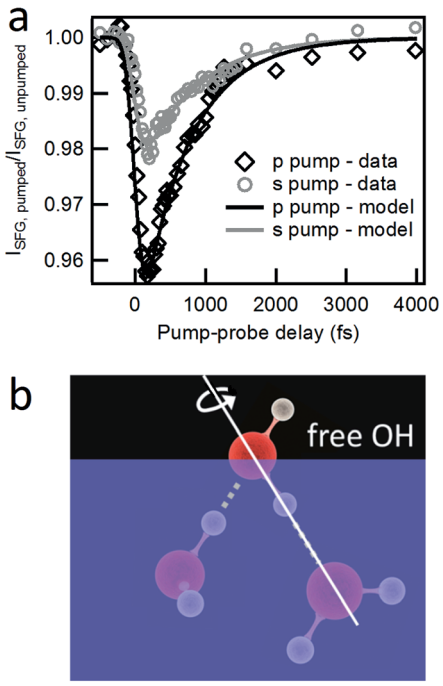

Figure 8. a) Time evolutions of the ratio of the pumped and unpumped SFG responses. The IR-SFG probe pulse is polarized along the P direction, explaining the larger signal observed under P-pumped conditions. Results from the numerical model calculation are given with black and gray lines. Reprinted with permission from Ref. [90]. Copyright 2011 by the American Physical Society. b) Schematic representation of the rotation of a free OH group at the H_2O–air interface.

It was found that, perhaps not completely unexpectedly, the reorientational motion of a water molecule with the free O–H bond is indeed fast and takes place on an approximately 1 ps timescale—that is, almost a factor of three faster than that of O–H groups in bulk water.[109] MD simulations[90] of this reorientational process revealed that, in contrast to the bulk, the reorientational dynamics at the interface occurs in a largely diffusive manner. Moreover, although in-plane and out-of-plane reorientational diffusion could not be disentangled experimentally, the simulation showed that in-plane and out-of-plane reorientational diffusion coefficients were comparable. This observation can be understood by noting that, although the free O–H is not hydrogen bonded, the other O–H group, within the same molecule, is. It would therefore be expected that the primary motion occurs as a rotation around the axis of the hydrogen-bonded O–H group (Figure 8b). This mechanism for reorientational motion of the free O–H group is consistent with both the diffusive nature of the motion, the inability to distinguish between in- and out-of-plane motions, and the faster-than-bulk reorientation.

It is also evident that, if the free O–H group reorients to a sufficiently large extent, it may become hydrogen-bonded. Likewise, previously hydrogen-bonded O–H groups at the interface may become free O–H groups, provided that sufficient time passes. Such structural dynamics can be resolved by exciting the free O–H group and probing the hydrogen-bonded O-H groups, and vice versa. If the free O–H group becomes hydrogen bonded, its vibrational frequency

will change, but the excitation will initially remain on that O–H group. Such experiments[93] indeed reveal that exchange occurs between the two sub-ensembles, on an approximately 1 ps timescale, which is consistent with the inferred reorientational dynamics.

This result also means that reorientational motion followed by hydrogen-bonding is one manner for the free O–H group to release excess vibrational energy into the bulk. The vibrational relaxation rate of O–H groups is known to be directly correlated with the hydrogen-bonding strength of the O–H group.[23,110] As a result, forming a hydrogen bond is a way for the free O–H groups to rapidly dissipate energy. Another way, which takes place on comparable timescales, is near-resonant energy transfer from the free O–H group to the other O–H group within the same water molecule. Both relaxation mechanisms—reorientation and energy transfer—allow the free O–H group to dissipate excess energy on sub-picosecond timescales,[93] which is orders of magnitude faster than, for example, non-hydrogen-bonded O–H groups on the silica surface,[11] making the water surface highly efficient at dissipating excess vibrational energy.

5.2. The Dynamics of Hydrogen-Bonded Interfacial Water Molecules

Vibrational energy transfer takes place not only between the free O–H and hydrogen-bonded O-H groups, but also among hydrogen-bonded O–H groups. This situation was first demonstrated for bulk water, and constitutes a rather unique property of water. In the bulk, very efficient vibrational energy transfer between O–H groups and rapid dissipation of the excess vibrational energy occurs. This is presumably one of the reasons why water is a good reaction medium; energy released in a chemical reaction can be transported away from the reactants very quickly, to avoid the back-reaction. The efficient energy transfer is, at least in part, the result of the very strong dipole–dipole interactions between the O–H groups, which allows excess vibrational energy to be delocalized over several O–H groups. Such vibrational energy transfer in bulk water has been studied in detail,[77,101,102,111,112] owing to the relevance of energy transfer in chemical processes occurring in water. Vibrational energy transfer in bulk water was first quantified by measuring the decay of the anisotropy that is induced using a linearly polarized excitation pulse as explained in the above Sections. Only those O–H groups that are aligned along the polarization axis of the excitation pulse will be excited. The anisotropy in the excitation distribution will decay owing to reorientational motion of water molecules as well as to vibrational energy exchange between O–H groups. It was shown that, for very strongly isotopically diluted O–H groups (i.e. HDO in D_2O), the anisotropy decay can be fully explained by reorientation of water molecules.[76,77] However, already at slightly higher, but still very low, HDO concentrations, energy transfer contributes significantly to the anisotropy decay.[77] Apparently, vibrational energy transfer between O–H groups is very efficient.[101,113–115]

Another method of quantifying energy transfer in water is by determining the time-dependence of the vibrational frequency of the O–H groups after excitation at one specific frequency. After excitation of a sub-set of O–H groups at one specific frequency, not only does the directionality become scrambled, but also the precise vibrational frequency. This phenomenon is called "spectral diffusion". In pure H_2O, spectral diffusion of the O–H stretch vibration occurs on an around 100 fs timescale.[101,102,116] This ultrafast timescale is too fast to be explained by time-dependent changes in the local hydrogen-bond strength, that is, structural relaxation,[115,117–120] and can be explained by near-resonant energy transfer to neighboring O–H groups,[113,121] with anharmonic coupling of the high-frequency O–H stretch to librational modes also contributing.[101,116]

Spectral diffusion in bulk water has been measured using 2D-IR spectroscopy.[101,102] For pure water H_2O, spectral diffusion by rapid hopping of the excitations from an O–H group to the other O–H group was found to occur on an approximately 100 fs timescale.[101,102] While initial time-resolved SFG experiments suggested that efficient energy transfer also occurred at the interface,[11,85] the effect of the interface on the rates and mechanisms of the energy transfer process was not explicitly studied until 2011. At that time, 2D-SFG spectra for D_2O recorded at different times after excitation ("tagging") were reported, allowing the interfacial energy dynamics of water to be probed specifically at the water–air interface.

These experiments showed that also at the water interface, very rapid energy exchange occurs, not only between free and hydrogen-bonded O–D groups, but also between hydrogen-bonded O–D groups. The energy transfer dynamics could be quantified using the time-dependent slope of the diagonal feature in the 2D-SFG experiments (see Figure 9). The initial slope at the delay time of $\tau = 0$ fs amounts to 0.23. The relatively small value for the initial slope may be due to a limited heterogeneity of the interfacial O–H stretch vibrations and/or a very rapid initial spectral diffusion arising from coupling to librational modes. The fact that the slope is non-zero indicates a preferential response at the excitation frequency; at short delay times, the water molecules still "remember" their vibrational frequency at the time of excitation. As the water molecules start to exchange vibrational energy, and given that they all have slightly different vibrational frequencies, the memory of the initial vibrational frequency is lost. In the 2D spectrum, this manifests itself as the slope going towards zero in the course of time. Interestingly, the fast dynamics observed at the water interface, could be fully explained by the reduced effective density at the interface. In bulk water, every O–H group is surrounded in all directions by other O–H groups, and energy transfer can occur in all directions, that is, over a 4π steradian solid angle. In contrast, at the surface there are only O–H groups below an interfacial O–H group. The probability of transferring vibrational energy is accordingly reduced at the interface, to a solid angle of 2π. This simple geometric effect accounts completely for the difference between energy transfer rates in the bulk and at the interface. Apparently, the structural dynamics of the hydrogen-bonded water molecules at the

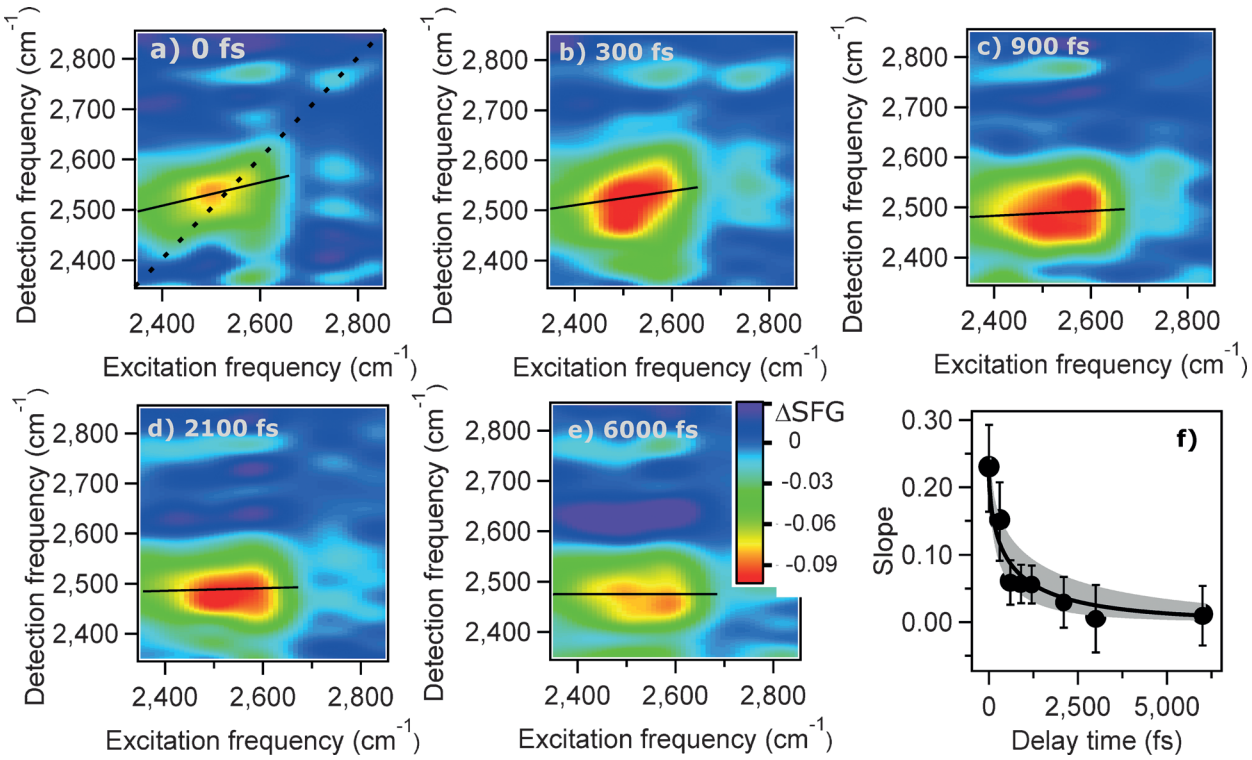

Figure 9. a)–e) 2D-SFG spectra as a function of delay time between excitation and detection for the D_2O–air interface. The black solid lines indicate the maxima in the 2D plots from which a gradient can be obtained. f) Gradient as a function of delay time. Experimental data are shown with black symbols. A model calculation accounting for spectral diffusion by resonant Förster energy transfer is shown as the solid line (shaded area indicates the relevant range of energy-transfer efficiencies). Figure taken from Ref. [100].

interface is not substantially different from those of water in the bulk—at least given the time resolution and signal-to-noise of these initial experiments.

5.3. Quantifying Structure from the Dynamics

For aqueous solutions containing surface-active solutes, the presence of solutes at the interface will further reduce the interfacial density of water molecules, by simple displacement of the water by the solute. The reduced density, in turn, will result in a reduction of the energy-transfer rate, as was previously shown using isotopic dilution experiments. Fewer O–H groups are present to accept the vibrational energy, as they are displaced by surface-active solutes. As such, a reduction in the interfacial vibrational energy transfer rate points to a surface propensity of solutes in aqueous solutions. This effect was used recently to quantify the surface propensity of halide anions in sodium halide solutions.[95] While previous experiments and simulations have indicated a strong surface propensity of iodide ions, and a moderate surface propensity of chloride anions, as is seen in Figure 10,[122] it has been very challenging to quantify the interfacial concentrations.

The interfacial ion concentration can be quantified from the reduction in the energy-transfer dynamics observed in 2D-SFG spectroscopy. Indeed, a marked decrease in the energy-transfer efficiency was observed for concentrated sodium halide solutions, as reflected by the leveling out of the decay of the slope of the central feature of the 2D-SFG spectrum (Figure 11). This directly demonstrates the surface propensity of both chloride and iodide ions. It is also apparent from the experiments that the change in slope is more pronounced for the iodide solutions, in agreement with previous experiments and simulations.

From these experiments, the effective interfacial water concentration can be determined, as the water concentration is directly related to the energy-transfer efficiency. We note that this interfacial water concentration is the average over

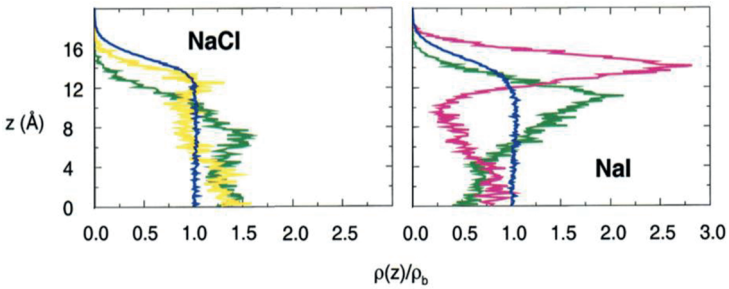

Figure 10. Axial profiles of the density, $\rho(z)$, with respect to the bulk density, ρ_b, for the water oxygen atoms and the ions for a 1.2 M NaCl (a) and NaI (b) solutions. The profiles for the sodium, chloride, and iodide ions are in green, yellow, and magenta, respectively, while the water oxygen profile is given in blue. Reprinted with permission from Ref. [122]. Copyright 2001 American Chemical Society.

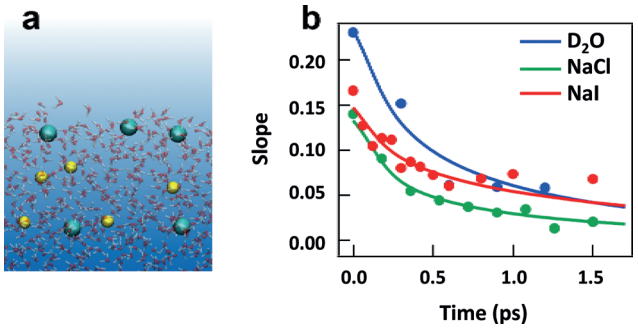

Figure 11. a) Schematic representation of the water–air interface in the presence of NaI. Na^+ and I^- ions are small yellow and large blue balls, respectively, together with the transparent images for the water molecules. b) Gradient decay obtained from 2D-SFG spectra in the OD vibrational region for three different solutions. The slower dynamics for the salt solutions illustrates the lower water concentration at the interface. From the reduced water concentration the interfacial ion concentration can be obtained. Figure taken from Ref. [95].

the approximately 6 Å total probing depth of the SFG spectroscopy. For the salt solutions, MD simulations have shown that the SFG spectrum does not change anymore after including water deeper than 6 Å from the interface, which is only slightly larger than the 5 Å for the pure water–air interface mentioned earlier.[48] Assuming that the reduction in the interfacial water concentration is due to displacement by ions at the interface, and armed with knowledge of the ionic radius of the different ions, the interfacial ion concentrations can be quantified in a straightforward manner. The results revealed a several-fold increase in the interfacial concentration compared to the bulk, testifying to the strong surface propensity of halide anions in solution.

6. MD Simulations as a Complementary Tool to Understand the Structure and Dynamics of Interfacial Water

MD simulations of the SFG response have been performed since 2000[55] and at present MD simulations are widely used for extracting the information on the structure and dynamics of the interfacial water from the SFG spectra.[123] The simulation technique has meanwhile been applied not only to the water–air interface[2,62,70,72,124] but also to the ice–air interface[71] and the water–lipid interface.[65] As described in pervious Sections, these theoretical efforts could reproduce the experimental SFG spectra quite accurately and provide molecular-level insight into the interfacial water structure, by revealing the molecular origin of the SFG peaks. Since the water–air interface is simple yet very heterogeneous, simulating the SFG spectra at this interface provides a critical check for the force field model of the ab initio based water molecules[125–127] as well as ab initio MD simulation.[128] Furthermore, we note that the extension of the SFG simulations to the 2D-SFG has been very important in interpreting the 2D spectra.[109,129] One obvious question theoretical 2D spectroscopy should address is the vibrational energy relaxation and the role of energy transfer from the interface to the bulk and from the bulk to the interface.

7. Outlook

7.1. SFG Spectroscopy of Other Water Vibrational Modes

As illustrated in this Review, the past years have witnessed tremendous progress in understanding the molecular structure and dynamics of the water–air interface using surface vibrational spectroscopic techniques. In this line of research the dominant mode under study has traditionally been the water O–H (or, equivalently, O–D) stretching mode. However, the steadily increasing laser output powers and tuning ranges extending even further into the IR, are enabling the study of weaker vibrational modes, such as the bending or the librational modes. These modes are interesting and relevant in their own right, and their study opens up a new dimension to the understanding of interfacial water. Following SFG combination band spectroscopy by the Borguet group,[130] the Benderskii group initiated the study on the interfacial H_2O bending mode[131] using SFG experiments. As a follow-up, MD simulations were combined with SFG experiments to identify the bending mode features and to obtain structural information from it.[132] The simulated $|\chi^{(2)}|^2$-spectrum is in agreement with the experimentally observed intensity spectrum, and the phase-sensitive $\mathrm{Im}[\chi^{(2)}]$ spectrum predicted by the simulation shows a negative feature at approximately 1650 cm^{-1} and a positive band at approximately 1730 cm^{-1} (see Figure 12). Note that the positive O–H stretch feature indicates the O–H group pointing up to the air, whereas the positive H-O-H bend feature indicates the

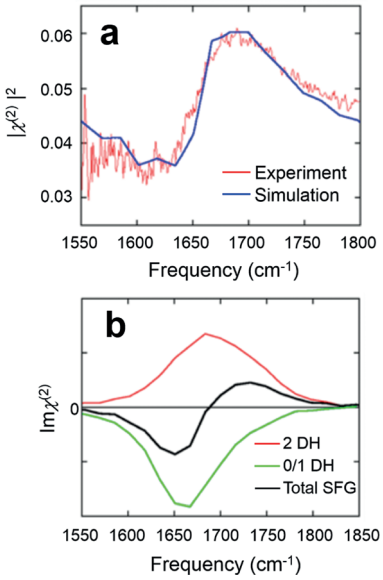

Figure 12. a) Experimental and simulated SFG intensities under SSP polarization in the bending-mode region. b) $\mathrm{Im}[\chi^{(2)}]$ spectra for subsets of water molecules having a different number of donor hydrogen atoms. Reprinted with permission from Ref. [132]. Copyright 2013 American Chemical Society.

C_2 symmetry axis pointing down to the bulk because of the opposite phase of the transition dipole moment and polarizability with respect to the bending motion.[132] The Im[$\chi^{(2)}$] spectrum of sub-ensembles of water (Figure 12b) indicates that water with the H-O-H C_2 symmetry axis pointing up to the air (negative Im[$\chi^{(2)}$]) originates from the water molecules having the free O–H on one side. In contrast, the C_2 symmetry axis of the water molecules with two hydrogen-bond donors points down into the bulk water. In this way, additional information on the structure of the interfacial water molecules is obtained. Furthermore, the precise frequency of the surface-active bending mode of water is important for understanding vibrational energy transfer from the O–H stretching mode to the lower frequency bending mode. This vibrational energy transfer occurs through the frequency overlap between the O–H stretching mode and overtone of the H-O-H bending mode in liquid water.[58] In this respect studying the low-frequency vibrational modes of water, the librational modes below 1000 cm^{-1}, would also be very interesting. Even more interesting, and also more challenging, would be to directly monitor the interfacial O–H···O hydrogen-bond stretching modes. While the O–H stretch serves as a good reporter, care has to be taken, as shown above, in converting the high-frequency SFG spectra into interfacial structures. As such, the hydrogen-bond stretching mode itself would provide quite direct information on the interfacial hydrogen-bonding geometries.

7.2. Nuclear Quantum Effects

Isotopic dilution experiments are generally performed and interpreted under the assumption that the structure of water is not substantially influenced by this isotopic dilution. However, a combined theoretical and experimental study of the free O–H/O–D groups at the water–air interface has shown that the bond orientation of the water molecules at this interface depends on the isotopic dilution which is caused by nuclear quantum effects.[133,134] Nuclear quantum effects arise because of the delocalization of especially low-mass particles owing to the quantum-mechanical nuclear wavefunction that describes the probability of finding the particle in a specific location. These give rise to the zero-point energy of the vibrational mode, influencing the hydrogen-bonding strength in a complex manner. Nuclear quantum effects are particularly relevant for the interface, because the vibrational energy difference between the free O–H and hydrogen-bond O–H stretch mode is comparable to kT at room temperature. If O-H groups are compared to O-D groups, the D atom is heavier and therefore more localized than the H atom, giving rise to competing effects: On the one hand, the larger uncertainty for the H atom destabilizes the hydrogen bond through the large intermolecular zero point energy, on the other hand, it stabilizes the hydrogen bond through the simultaneous intramolecular zero point energy in bulk liquid water.[135] These effects are responsible, for example, for the higher melting point of D_2O ice than H_2O ice. Although nuclear quantum effects on bulk properties have been extensively studied,[136] the effects on the structure of the aqueous interface has been addressed only very recently.[137,138] Path integral MD simulations at the water–air interface revealed the preferential orientation of the O–H and O–D groups of the HDO molecule. The average orientational angle between the O–H (O–D) groups and the surface normal is displayed in Figure 13b. The simulated and experimental SFG data confirmed that the O–H group of an HDO molecule is slightly more oriented toward the air and is less inclined to engage in hydrogen bonds with other water molecules (Figure 13c). The O–D group of the same molecule prefers to orient towards the bulk to form hydrogen bonds. In contrast, pure H_2O and D_2O show an indistinguishable angular distribution. The preferential orientation of HDO molecules, with its O-H group sticking out of the surface, while H_2O and D_2O behave similarly to each other, shows that the symmetry breaking in the HDO molecules arising from the nuclear quantum effects causes an asymmetric tendency to form hydrogen bonds. This finding is important to understand the vapor–water equilibration for

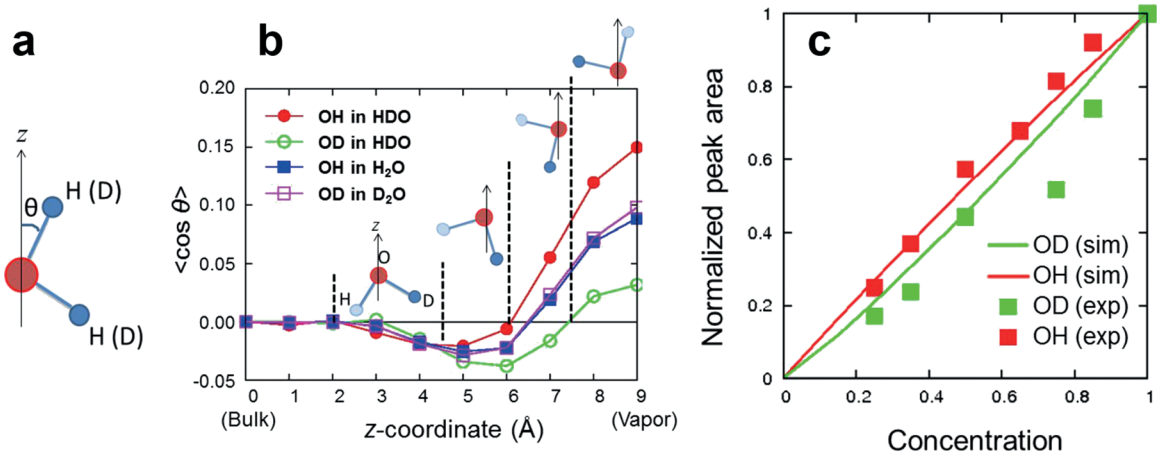

Figure 13. a) Schematic picture of the angle θ formed by the O–H (O–D) bond and the surface normal pointing to the vapor region. b) Axial distribution of $\langle\cos\theta\rangle$. c) Normalized free O–H (O–D) stretch band in the SFG spectrum as a function of the concentration of H_2O (D_2O) in the H_2O–D_2O mixture. Reprinted with permission from Ref. [137]. Copyright 2012 by the American Physical Society.

the H_2O/D_2O mixture[139] as well as to investigate fundamental effects associated with nuclear quantum effects, in particular near interfaces.[138,140]

7.3. Towards Complex Interfaces

Of course SFG spectroscopy can be used for many other aqueous interfaces other than the water–air interface. Indeed, since its development, it has been used on more complex aqueous interfaces than "just" the water–air interface: for example, water interfacing with hydrophobic materials,[12,15,141] water–lipid interfaces as model membranes,[142–145] water–glass interfaces,[146–150] and aqueous protein interfaces.[151,152] Moreover, owing to the development of SFG scattering, also aqueous non-planar interfaces can be studied.[153] From these experiments information on, for example, the ordering of water underneath charged lipids, the ordering of lipids themselves, the orientation of water in contact with a glass, has been obtained. All these systems can be measured under static conditions or the system can be disturbed in a certain way and the effect of the perturbation can be unraveled. The perturbation can be chemical, that is, by injecting peptides into the aqueous phase underneath a lipid monolayer and following their interaction with the lipids, or physical, that is, changing temperature or pressure.

Herein, we briefly show a recent application of SFG, in which SFG was used to study a non-equilibrium interfacial aqueous system: water flowing along a mineral surface.[154,155] The question that motivated this research was: How is the interfacial organization affected when water flows along a surface? In the standard continuum model of flow, a "stick boundary condition" is generally assumed, which implies that the water organization at the interface would remain unchanged in the presence or absence of flow. Figure 14a shows that this is not what is observed experimentally: the SFG signal of water in contact with a CaF_2 window under static conditions (flow off) and under perturbation by a laminar flow (flow on). Surprisingly, the SFG signal increases by a factor of two upon switching on the flow. After switching off the flow the signal equilibrates back to the flow off state. As evident from Figure 14b, the flow-induced changes and the recovery are reproducible over many flow on/off cycles. Similarly, for water in contact with an SiO_2 window, equally dramatic changes in the SFG signal could be observed.[154] From a set of experiments with varying aqueous solutions, it could be concluded that the flow washes away ions dissolved from the solid material, which reside in the interfacial region. As a result the dissolution equilibrium reaction is biased to one side and the surface charge changes. Remarkably, to achieve a similar change in the surface charge as affected by flow, by changing the pH value, requires a 2–3 pH unit change under static conditions. These results showed that the flow significantly perturbs the chemistry at the surface.

Clearly, the methodology of SFG has been developed to such an extent that detailed studies, with high temporal and even spatial resolution[156,157] can now be applied to highly complex interfaces. It will be exciting to see how the application of some of the advanced spectroscopic applications described herein in detail for the water–air interface will be able to answer important questions in, for example, (photo-)catalysis on much more complex, but accordingly more relevant, aqueous and ice surfaces.

7.4. Non-Surface-Specific Vibrational Spectroscopy used for Understating Interfacial Molecular Structure and Dynamics

We have limited ourselves in this Review to SFG studies on the planar water–air interface. However, non-surface-specific vibrational techniques, such as IR spectroscopy, may provide comparable insights by minimizing the bulk contribution and maximizing the surface contribution. Excellent sample to maximize the surface contribution are reverse micelles in which water is present inside the micelle. By varying the water/surfactant ratio, the size of the micelles and therefore the amount of surface water can be controlled. Time-resolved IR spectroscopy has been used to study reverse micelles,[158–162] through which it has been found that the reorientational dynamics of the water molecules adjacent to the hydrophilic headgroup of a surfactant slows down compared with the bulk water. However, we should note that these water molecules surrounded by surfactant molecules

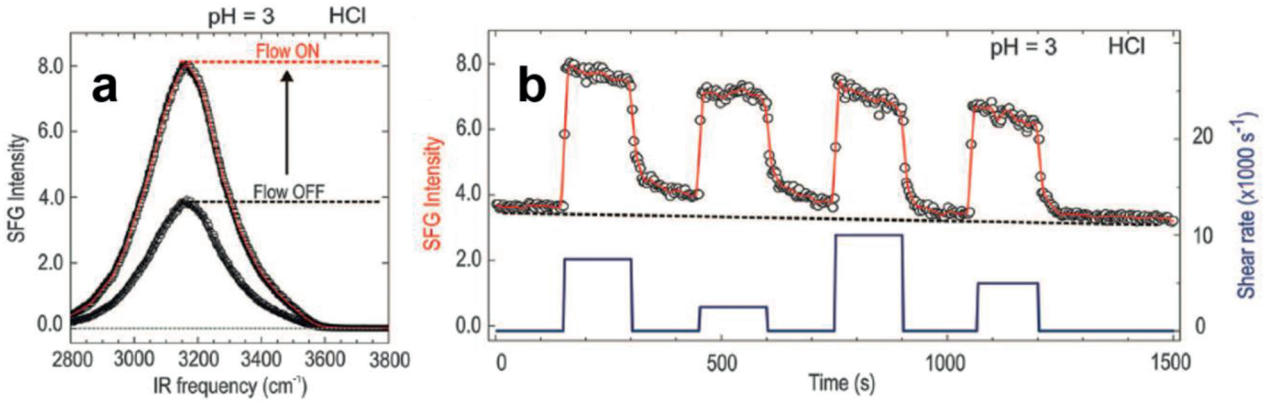

Figure 14. a) SFG spectrum for the water–CaF_2 interface at pH of 3 with the flow off and on. b) SFG intensity as a function of the shear rate. From Ref. [154]. Reprinted with permission from AAAS.

are confined in three dimensions. In contrast, water at an aqueous interface is one-dimensionally confined, and thus may be fundamentally different from water in three-dimensionally confined geometries.

Acknowledgement

We would like to thank J. Hunger for commenting on the manuscript and H. S. Varol and S. H. Parekh for sharing their Raman results. All co-workers and collaborators that have contributed to this work over the years are also gratefully acknowledged.

How to cite: *Angew. Chem. Int. Ed.* **2015**, *54*, 5560–5576
Angew. Chem. **2015**, *127*, 5652–5669

[1] D. Laage, J. T. Hynes, *Science* **2006**, *311*, 832–835.
[2] P. A. Pieniazek, C. J. Tainter, J. L. Skinner, *J. Am. Chem. Soc.* **2011**, *133*, 10360–10363.
[3] K. Liu, M. G. Brown, C. Carter, R. J. Saykally, J. K. Gregory, D. C. Clary, *Nature* **1996**, *381*, 501.
[4] J. Dash, A. Rempel, J. Wettlaufer, *Rev. Mod. Phys.* **2006**, *78*, 695–741.
[5] G. E. Brown, V. E. Henrich, W. H. Casey, D. L. Clark, C. Eggleston, A. Felmy, D. W. Goodman, M. Grätzel, G. Maciel, M. I. McCarthy, K. H. Nealson, D. A. Sverjensky, M. F. Toney, J. M. Zachara, *Chem. Rev.* **1999**, *99*, 77–174.
[6] J. Wettlaufer, *Phys. Rev. Lett.* **1999**, *82*, 2516–2519.
[7] J. S. Wettlaufer, *Philos. Trans. R. Soc. London Ser. A* **1999**, *357*, 3403–3425.
[8] J. H. Seinfeld, S. N. Pandis, *Atmospheric Chemistry and Physics*: *From Air Pollution to Climate Change*, Wiley, New York, **1998**.
[9] L. F. Scatena, M. G. Brown, G. L. Richmond, *Science* **2001**, *292*, 908–912.
[10] S. Ye, S. Nihonyanagi, K. Uosaki, *Phys. Chem. Chem. Phys.* **2001**, *3*, 3463.
[11] J. A. McGuire, Y. R. Shen, *Science* **2006**, *313*, 1945–1948.
[12] C. S. Tian, Y. R. Shen, *Proc. Natl. Acad. Sci. USA* **2009**, *106*, 15148–15153.
[13] R. Scheu, B. M. Rankin, Y. Chen, K. C. Jena, D. Ben-Amotz, S. Roke, *Angew. Chem.* **2014**, *126*, 9714–9717.
[14] J.-S. Samson, R. Scheu, N. Smolentsev, S. W. Rick, S. Roke, *Chem. Phys. Lett.* **2014**, *615*, 124–131.
[15] S. W. Rick, P. Jungwirth, A. G. F. De Beer, H. B. De Aguiar, J. Samson, S. Roke, *J. Am. Chem. Soc.* **2011**, *133*, 10204–10210.
[16] S. Strazdaite, J. Versluis, E. H. G. Backus, H. J. Bakker, *J. Chem. Phys.* **2014**, *140*, 054711.
[17] E. Tyrode, M. W. Rutland, C. D. Bain, *J. Am. Chem. Soc.* **2008**, *130*, 17434–17445.
[18] P. Wernet, D. Nordlund, U. Bergmann, M. Cavalleri, M. Odelius, H. Ogasawara, L. A. Näslund, T. K. Hirsch, L. Ojamäe, P. Glatzel, L. G. M. Pettersson, A. Nilsson, *Science* **2004**, *304*, 995–999.
[19] M. Leetmaa, K. T. Wikfeldt, M. P. Ljungberg, M. Odelius, J. Swenson, A. Nilsson, L. G. M. Pettersson, *J. Chem. Phys.* **2008**, *129*, 084502.
[20] Z. Zhang, P. Fenter, L. Cheng, N. C. Sturchio, M. J. Bedzyk, M. Předota, A. Bandura, J. D. Kubicki, S. N. Lvov, P. T. Cummings, A. A. Chialvo, M. K. Ridley, P. Bénézeth, L. Anovitz, D. A. Palmer, M. L. Machesky, D. J. Wesolowski, *Langmuir* **2004**, *20*, 4954–4969.
[21] C. Park, P. Fenter, N. Sturchio, J. Regalbuto, *Phys. Rev. Lett.* **2005**, *94*, 076104.
[22] E. Mamontov, D. J. Wesolowski, L. Vlcek, P. T. Cummings, J. Rosenqvist, W. Wang, D. R. Cole, *J. Phys. Chem. C* **2008**, *112*, 12334–12341.
[23] R. Rey, K. B. Møller, J. T. Hynes, *J. Phys. Chem. A* **2002**, *106*, 11993–11996.
[24] R. Kumar, J. Schmidt, J. Skinner, *J. Chem. Phys.* **2007**, *126*, 204107.
[25] B. M. Auer, J. L. Skinner, *J. Chem. Phys.* **2008**, *128*, 224511.
[26] B. M. Auer, R. Kumar, J. R. Schmidt, J. L. Skinner, *Proc. Natl. Acad. Sci. USA* **2007**, *104*, 14215–14220.
[27] J. J. Loparo, S. T. Roberts, R. A. Nicodemus, A. Tokmakoff, *Chem. Phys.* **2007**, *341*, 218–229.
[28] Y. R. Shen, *Nature* **1989**, *337*, 519.
[29] Q. Du, R. Superfine, E. Freysz, Y. R. Shen, *Phys. Rev. Lett.* **1993**, *70*, 2313–2316.
[30] Q. Du, E. Freysz, Y. R. Shen, *Science* **1994**, *264*, 826.
[31] Q. Du, E. Freysz, Y. R. Shen, *Phys. Rev. Lett.* **1994**, *72*, 238–241.
[32] G. L. Richmond, *Chem. Rev.* **2002**, *102*, 2693–2724.
[33] D. E. Gragson, G. L. Richmond, *J. Phys. Chem. B* **1998**, *102*, 3847–3861.
[34] E. A. Raymond, G. L. Richmond, *J. Phys. Chem. B* **2004**, *108*, 5051–5059.
[35] E. A. Raymond, T. L. Tarbuck, M. G. Brown, G. L. Richmond, *J. Phys. Chem. B* **2003**, *107*, 546–556.
[36] T. L. Tarbuck, G. L. Richmond, *J. Am. Chem. Soc.* **2005**, *127*, 16806–16807.
[37] T. L. Tarbuck, S. T. Ota, G. L. Richmond, *J. Am. Chem. Soc.* **2006**, *128*, 14519–14527.
[38] Y. R. Shen, V. Ostroverkhov, *Chem. Rev.* **2006**, *106*, 1140–1154.
[39] S. Kataoka, M. C. Gurau, F. Albertorio, M. A. Holden, S. Lim, R. D. Yang, P. S. Cremer, *Langmuir* **2004**, *20*, 1662–1666.
[40] S. Baldelli, *J. Phys. Chem. B* **2003**, *107*, 6148–6152.
[41] J. Liu, J. C. Conboy, *J. Am. Chem. Soc.* **2004**, *126*, 8376–8377.
[42] W. Gan, D. Wu, Z. Zhang, R. Feng, H. Wang, *J. Chem. Phys.* **2006**, *124*, 114705.
[43] S. Gopalakrishnan, P. Jungwirth, D. J. Tobias, H. C. Allen, *J. Phys. Chem. B* **2005**, *109*, 8861–8872.
[44] W. Zhang, D. Zheng, Y. Xu, H. Bian, Y. Guo, H. Wang, *J. Chem. Phys.* **2005**, *123*, 224713.
[45] S. Gopalakrishnan, D. Liu, H. C. Allen, M. Kuo, M. J. Shultz, *Chem. Rev.* **2006**, *106*, 1155–1175.
[46] L. M. Levering, M. R. Sierra-Hernandez, H. C. Allen, *J. Phys. Chem. C* **2007**, *111*, 8814–8826.
[47] E. Whalley, *Can. J. Chem.* **1977**, *55*, 3429.
[48] T. Ishiyama, A. Morita, *J. Phys. Chem. C* **2007**, *111*, 721–737.
[49] T. Ishiyama, A. Morita, *J. Phys. Chem. C* **2007**, *111*, 738–748.
[50] R. Feng, Y. Guo, L. Velarde, H. Wang, *J. Phys. Chem. A* **2011**, *115*, 6015–6027.
[51] V. Buch, T. L. Tarbuck, G. L. Richmond, H. Groenzin, I. Li, M. J. Shultz, *J. Chem. Phys.* **2007**, *127*, 204710.
[52] V. Buch, *J. Phys. Chem. B* **2005**, *109*, 17771–17774.
[53] D. S. Walker, D. K. Hore, G. L. Richmond, *J. Phys. Chem. B* **2006**, *110*, 20451–20459.
[54] R. Rosenberg, *Phys. Today* **2005**, *58*, 50–55.
[55] A. Morita, J. T. Hynes, *Chem. Phys.* **2000**, *258*, 371–390.
[56] A. Sokołowska, *J. Raman Spectrosc.* **1991**, *22*, 31–33.
[57] O. Henri-Rousseau, P. Blaise, D. Chamma, *Adv. Chem. Phys.* **2002**, *121*, 241–310.
[58] S. Ashihara, N. Huse, A. Espagne, E. Nibbering, T. Elsaesser, *Chem. Phys. Lett.* **2006**, *424*, 66–70.
[59] E. A. Raymond, T. L. Tarbuck, G. L. Richmond, *J. Phys. Chem. B* **2002**, *106*, 2817–2820.
[60] M. Sovago, R. K. Campen, G. Wurpel, M. Müller, H. J. Bakker, M. Bonn, *Phys. Rev. Lett.* **2008**, *100*, 173901.
[61] M. Sovago, R. K. Campen, H. J. Bakker, M. Bonn, *Chem. Phys. Lett.* **2009**, *470*, 7–12.

[62] S. Nihonyanagi, T. Ishiyama, T.-K. Lee, S. Yamaguchi, M. Bonn, A. Morita, T. Tahara, *J. Am. Chem. Soc.* **2011**, *133*, 16875 – 16880.
[63] M. Bonn, H. J. Bakker, Y. Tong, E. H. G. Backus, *Biointerphases* **2012**, *7*, 20.
[64] T. Ishiyama, A. Morita, *J. Phys. Chem. C* **2009**, *113*, 16299 – 16302.
[65] Y. Nagata, S. Mukamel, *J. Am. Chem. Soc.* **2010**, *132*, 6434 – 6442.
[66] B. M. Auer, J. L. Skinner, *J. Chem. Phys.* **2008**, *129*, 214705.
[67] S. Nihonyanagi, S. Yamaguchi, T. Tahara, *J. Chem. Phys.* **2009**, *130*, 204704.
[68] V. Ostroverkhov, G. Waychunas, Y. R. Shen, *Phys. Rev. Lett.* **2005**, *94*, 2 – 5.
[69] C. Tian, Y. R. Shen, *J. Am. Chem. Soc.* **2009**, *131*, 2790 – 2791.
[70] T. Ishiyama, A. Morita, *J. Phys. Chem. C* **2009**, *113*, 16299 – 16302.
[71] T. Ishiyama, H. Takahashi, A. Morita, *J. Phys. Chem. Lett.* **2012**, *3*, 3001 – 3006.
[72] P. A. Pieniazek, C. J. Tainter, J. L. Skinner, *J. Chem. Phys.* **2011**, *135*, 044701.
[73] I. V. Stiopkin, C. Weeraman, P. A. Pieniazek, F. Y. Shalhout, J. L. Skinner, A. V. Benderskii, *Nature* **2011**, *474*, 192 – 195.
[74] M. Cho, *Chem. Rev.* **2008**, *108*, 1331 – 1418.
[75] T. Schäfer, J. Lindner, P. Vöhringer, D. Schwarzer, *J. Chem. Phys.* **2009**, *130*, 224502.
[76] H. J. Bakker, J. L. Skinner, *Chem. Rev.* **2010**, *110*, 1498 – 1517.
[77] S. Woutersen, H. J. Bakker, *Nature* **1999**, *402*, 507 – 509.
[78] P. Hamm, M. T. Zanni, *Concepts and Methods of 2D Infrared Spectroscopy*, Cambridge University Press, Cambridge, **2011**.
[79] Ł. Szyc, M. Yang, E. T. J. Nibbering, T. Elsaesser, *Angew. Chem. Int. Ed.* **2010**, *49*, 3598 – 3610; *Angew. Chem.* **2010**, *122*, 3680 – 3693.
[80] M. D. Fayer, *Ultrafast Infrared Vibrational Spectroscopy*, CRC, Boca Raton, **2013**.
[81] A. A. Bakulin, C. Liang, T. L. C. Jansen, D. A. Wiersma, H. J. Bakker, M. S. Pshenichnikov, *Acc. Chem. Res.* **2009**, *42*, 1229.
[82] J. D. Eaves, J. J. Loparo, C. J. Fecko, S. T. Roberts, A. Tokmakoff, P. L. Geissler, *Proc. Natl. Acad. Sci. USA* **2005**, *102*, 13019 – 13022.
[83] J. B. Asbury, T. Steinel, K. Kwak, S. A. Corcelli, C. P. Lawrence, J. L. Skinner, M. D. Fayer, *J. Chem. Phys.* **2004**, *121*, 12431 – 12446.
[84] J. B. Asbury, T. Steinel, C. Stromberg, S. A. Corcelli, C. P. Lawrence, J. L. Skinner, M. D. Fayer, *J. Phys. Chem. A* **2004**, *108*, 1107 – 1119.
[85] M. Smits, A. Ghosh, M. Sterrer, M. Müller, M. Bonn, *Phys. Rev. Lett.* **2007**, *98*, 098302.
[86] A. Ghosh, M. Smits, J. Bredenbeck, M. Bonn, *J. Am. Chem. Soc.* **2007**, *129*, 9608 – 9609.
[87] J. Bredenbeck, A. Ghosh, M. Smits, M. Bonn, *J. Am. Chem. Soc.* **2008**, *130*, 2152 – 2153.
[88] A. Eftekhari-Bafrooei, E. Borguet, *J. Am. Chem. Soc.* **2010**, *132*, 3756 – 3761.
[89] J. E. Laaser, W. Xiong, M. T. Zanni, *J. Phys. Chem. B* **2011**, *115*, 2536 – 2546.
[90] C.-S. Hsieh, R. K. Campen, A. C. V. Verde, P. Bolhuis, H.-K. Nienhuys, M. Bonn, *Phys. Rev. Lett.* **2011**, *107*, 116102.
[91] P. C. Singh, S. Nihonyanagi, S. Yamaguchi, T. Tahara, *J. Chem. Phys.* **2012**, *137*, 094706.
[92] P. C. Singh, S. Nihonyanagi, S. Yamaguchi, T. Tahara, *J. Chem. Phys.* **2013**, *139*, 161101.
[93] C.-S. Hsieh, R. K. Campen, M. Okuno, E. H. G. Backus, Y. Nagata, M. Bonn, *Proc. Natl. Acad. Sci. USA* **2013**, *110*, 18780 – 18785.
[94] C.-S. Hsieh, M. Okuno, J. Hunger, E. H. G. Backus, Y. Nagata, M. Bonn, *Angew. Chem. Int. Ed.* **2014**, *53*, 8146 – 8149; *Angew. Chem.* **2014**, *126*, 8284 – 8288.
[95] L. Piatkowski, Z. Zhang, E. H. G. Backus, H. J. Bakker, M. Bonn, *Nat. Commun.* **2014**, *5*, 4083.
[96] S. Mukamel, *Annu. Rev. Phys. Chem.* **2000**, *51*, 691 – 729.
[97] R. R. Ernst, G. Bodenhausen, A. Wokaun, *Principles of Nuclear Magnetic Resonance in One and Two Dimensions*, Clarendon, **1990**.
[98] J. Bredenbeck, A. Ghosh, H. Nienhuys, M. Bonn, *Acc. Chem. Res.* **2009**, *42*, 1332 – 1342.
[99] W. Xiong, J. E. Laaser, R. D. Mehlenbacher, M. T. Zanni, *Proc. Natl. Acad. Sci. USA* **2011**, *108*, 20902 – 20907.
[100] Z. Zhang, L. Piatkowski, H. J. Bakker, M. Bonn, *Nat. Chem.* **2011**, *3*, 888 – 893.
[101] M. L. Cowan, B. D. Bruner, N. Huse, J. R. Dwyer, B. Chugh, E. T. J. Nibbering, T. Elsaesser, R. J. D. Miller, *Nature* **2005**, *434*, 199 – 202.
[102] K. Ramasesha, L. De Marco, A. Mandal, A. Tokmakoff, *Nat. Chem.* **2013**, *5*, 935 – 940.
[103] X. Chen, T. Yang, S. Kataoka, P. S. Cremer, *J. Am. Chem. Soc.* **2007**, *129*, 12272 – 12279.
[104] Y. Jung, R. A. Marcus, *J. Am. Chem. Soc.* **2007**, *129*, 5492 – 5502.
[105] D. Chandler, *Nature* **2005**, *437*, 640 – 647.
[106] S. Narayan, J. Muldoon, M. G. Finn, V. V. Fokin, H. C. Kolb, K. B. Sharpless, *Angew. Chem. Int. Ed.* **2005**, *44*, 3275 – 3279; *Angew. Chem.* **2005**, *117*, 3339 – 3343.
[107] B. Braunschweig, S. Eissner, W. Daum, *J. Phys. Chem. C* **2008**, *112*, 1751 – 1754.
[108] H. J. Bakker, Y. L. A. Rezus, R. L. A. Timmer, *J. Phys. Chem. A* **2008**, *112*, 11523 – 11534.
[109] Y. Ni, S. M. Gruenbaum, J. L. Skinner, *Proc. Natl. Acad. Sci. USA* **2013**, *110*, 1992 – 1998.
[110] K. B. Møller, R. Rey, J. T. Hynes, *J. Phys. Chem. A* **2004**, *108*, 1275 – 1289.
[111] S. Imoto, S. S. Xantheas, S. Saito, *J. Chem. Phys.* **2013**, *139*, 044503.
[112] J. Lindner, P. Vöhringer, M. S. Pshenichnikov, D. Cringus, D. A. Wiersma, M. Mostovoy, *Chem. Phys. Lett.* **2006**, *421*, 329 – 333.
[113] L. Piatkowski, K. B. Eisenthal, H. J. Bakker, *Phys. Chem. Chem. Phys.* **2009**, *11*, 9033 – 9038.
[114] C. J. Fecko, J. J. Loparo, S. T. Roberts, A. Tokmakoff, *J. Chem. Phys.* **2005**, *122*, 054506.
[115] T. Steinel, J. B. Asbury, J. Zheng, M. D. Fayer, *J. Phys. Chem. A* **2004**, *108*, 10957 – 10964.
[116] D. Kraemer, M. L. Cowan, A. Paarmann, N. Huse, E. T. J. Nibbering, T. Elsaesser, R. J. D. Miller, *Proc. Natl. Acad. Sci. USA* **2008**, *105*, 437 – 442.
[117] R. Laenen, C. Rauscher, A. Laubereau, *Phys. Rev. Lett.* **1998**, *80*, 2622 – 2625.
[118] G. Gale, G. Gallot, F. Hache, N. Lascoux, S. Bratos, J. C. Leicknam, *Phys. Rev. Lett.* **1999**, *82*, 1068 – 1071.
[119] S. Woutersen, H. J. Bakker, *Phys. Rev. Lett.* **1999**, *83*, 2077 – 2080.
[120] C. P. Lawrence, J. L. Skinner, *J. Chem. Phys.* **2003**, *118*, 264.
[121] S. Woutersen, H. J. Bakker, *Nature* **1999**, *402*, 507 – 509.
[122] P. Jungwirth, D. J. Tobias, *J. Phys. Chem. B* **2001**, *105*, 10468 – 10472.
[123] T. Ishiyama, T. Imamura, A. Morita, *Chem. Rev.* **2014**, *114*, 8447.
[124] B. M. Auer, J. L. Skinner, *J. Phys. Chem. B* **2009**, *113*, 4125 – 4130.
[125] G. S. Fanourgakis, S. S. Xantheas, *J. Chem. Phys.* **2008**, *128*, 074506.
[126] T. Hasegawa, Y. Tanimura, *J. Phys. Chem. B* **2011**, *115*, 5545 – 5553.

[127] G. R. Medders, V. Babin, F. Paesani, *J. Chem. Theory Comput.* **2013**, *9*, 1103.
[128] M. Sulpizi, M. Salanne, M. Sprik, M.-P. Gaigeot, *J. Phys. Chem. Lett.* **2013**, *4*, 83.
[129] Y. Nagata, S. Mukamel, *J. Am. Chem. Soc.* **2011**, *133*, 3276 – 3279.
[130] O. Isaienko, S. Nihonyanagi, D. Sil, E. Borguet, *J. Phys. Chem. Lett.* **2013**, *4*, 531.
[131] M. Vinaykin, A. V. Benderskii, *J. Phys. Chem. Lett.* **2012**, *3*, 3348.
[132] Y. Nagata, C.-S. Hsieh, T. Hasegawa, J. Voll, E. H. G. Backus, M. Bonn, *J. Phys. Chem. Lett.* **2013**, *4*, 1872 – 1877.
[133] D. Chandler, P. Wolynes, *J. Chem. Phys.* **1981**, *74*, 4078.
[134] R. P. Feynman, *Rev. Mod. Phys.* **1948**, *20*, 367.
[135] S. Habershon, T. E. Markland, D. E. Manolopoulos, *J. Chem. Phys.* **2009**, *131*, 024501.
[136] M. Ceriotti, J. Cuny, M. Parrinello, D. E. Manolopoulos, *Proc. Natl. Acad. Sci. USA* **2013**, *110*, 15591 – 15596.
[137] Y. Nagata, R. E. Pool, E. H. G. Backus, M. Bonn, *Phys. Rev. Lett.* **2012**, *109*, 226101.
[138] J. Liu, R. S. Andino, C. M. Miller, X. Chen, D. M. Wilkins, M. Ceriotti, D. E. Manolopoulos, *J. Phys. Chem. C* **2013**, *117*, 2944.
[139] T. E. Markland, B. J. Berne, *Proc. Natl. Acad. Sci. USA* **2012**, *109*, 7988 – 7991.
[140] X.-Z. Li, M. I. J. Probert, A. Alavi, A. Michaelides, *Phys. Rev. Lett.* **2010**, *104*, 066102.
[141] F. G. Moore, G. L. Richmond, *Acc. Chem. Res.* **2008**, *41*, 739.
[142] E. Tyrode, C. M. Johnson, M. W. Rutland, P. M. Claesson, *J. Phys. Chem. C* **2007**, *111*, 11642 – 11652.
[143] X. Chen, H. C. Allen, *J. Phys. Chem. A* **2009**, *113*, 12655 – 12662.
[144] X. Chen, W. Hua, Z. Huang, H. C. Allen, *J. Am. Chem. Soc.* **2010**, *43210*, 154.
[145] C. M. Johnson, S. Baldelli, *Chem. Rev.* **2014**, *114*, 8416 – 8446.
[146] S. C. Flores, J. Kherb, N. Konelick, X. Chen, P. S. Cremer, *J. Phys. Chem. C* **2012**, *116*, 5730 – 5734.
[147] P. A. Covert, K. C. Jena, D. K. Hore, *J. Phys. Chem. Lett.* **2014**, *5*, 143 – 148.
[148] K. A. Becraft, G. L. Richmond, *Langmuir* **2001**, *17*, 7721 – 7724.
[149] K. C. Jena, D. K. Hore, *J. Phys. Chem. C* **2009**, *113*, 15364 – 15372.
[150] K. C. Jena, P. A. Covert, D. K. Hore, *J. Phys. Chem. Lett.* **2011**, *2*, 1056 – 1061.
[151] L. Fu, G. Ma, E. C. Y. Yan, *J. Am. Chem. Soc.* **2010**, *132*, 5405 – 5412.
[152] D. Schach, C. Globisch, S. J. Roeters, S. Woutersen, A. Fuchs, C. K. Weiss, E. H. G. Backus, K. Landfester, M. Bonn, C. Peter, T. Weidner, *J. Chem. Phys.* **2014**, *141*, 22D517.
[153] S. Roke, G. Gonella, *Annu. Rev. Phys. Chem.* **2012**, *63*, 353 – 378.
[154] D. Lis, E. H. G. Backus, J. Hunger, S. H. Parekh, M. Bonn, *Science* **2014**, *344*, 1138 – 1142.
[155] G. A. Waychunas, *Science* **2014**, *344*, 1094 – 1095.
[156] V. Raghunathan, Y. Han, O. Korth, N. Ge, E. O. Potma, *Opt. Lett.* **2011**, *36*, 3891 – 3893.
[157] J. H. Jang, J. Jacob, G. Santos, T. R. Lee, S. Baldelli, *J. Phys. Chem. C* **2013**, *117*, 15192 – 15202.
[158] E. E. Fenn, D. B. Wong, M. D. Fayer, *Proc. Natl. Acad. Sci. USA* **2009**, *106*, 15243.
[159] T. H. van der Loop, M. R. Panman, S. Lotze, J. Zhang, T. Vad, H. J. Bakker, W. F. C. Sager, S. Woutersen, *J. Chem. Phys.* **2012**, *137*, 044503.
[160] D. Cringus, A. Bakulin, P. Vo, M. S. Pshenichnikov, D. A. Wiersma, *J. Phys. Chem. B* **2007**, *111*, 14193 – 14207.
[161] N. E. Levinger, R. Costard, E. T. J. Nibbering, T. Elsaesser, *J. Phys. Chem. A* **2011**, *115*, 11952 – 11959.
[162] D. E. Moilanen, E. E. Fenn, D. Wong, M. D. Fayer, *J. Chem. Phys.* **2009**, *131*, 014704.
[163] P. L. Geissler, *Ann. Rev. Phys. Chem.* **2013**, *64*, 317 – 337.
[164] C. S. Tian, Y. R. Shen, *Surf. Sci. Rep.* **2014**, *69*, 105 – 131.

Received: November 18, 2014
Published online: April 15, 2015